*Journal of Chromatography*, 512 (1990) 101–114
Elsevier Science Publishers B.V., Amsterdam

CHROMSYMP. 1967

# High-performance liquid chromatography of amino acids, peptides and proteins

## CIII[a]. Mass transfer resistances in ion-exchange and dye-affinity chromatography of proteins

A. JOHNSTON and M. T. W. HEARN*
*Department of Biochemistry and Centre for Bioprocess Technology, Monash University, Clayton, Melbourne, Victoria 3168 (Australia)*

ABSTRACT

Adsorption equilibria and rate kinetics have been investigated for the binding of several proteins, with different molecular geometries, to several ion-exchange and dye-affinity chromatographic resins with varying pore size and protein accessibilities. The pore geometry was shown to play a significant role in the protein capacity and loadability of both the ion-exchange and dye-affinity resins. For example the Fractogel HW75–Cibacron Blue F3GA affinity sorbent had the greatest capacity for the small protein, lysozyme, compared to the other Fractogel HW-Cibacron Blue F3GA sorbents, and similarly, the ion-exchange resins, such as DEAE-Fractogel 65, bound more human serum albumin (HSA), as opposed to the larger protein, ferritin.

The apparent diffusion of protein from the bulk phase to the ligands/ionic sites was calculated to be considerably restricted when the pore to protein size ratio was small, as is the case of DEAE Fractogel 65/ferritin system, and the dye-affinity Fractogel HW55/HSA system. In these circumstances, pore diffusivity was calculated to be up to 100-fold smaller than bulk diffusivity.

## INTRODUCTION

The purification of a specific protein involves a cascade of chromatographic processes, each step harnessing a unique biological or chemical property to separate the desired component from its contaminants in the crude mixture. Ion-exchange chromatography (IEC) is predominantly used in the initial stages as a reliable method of volume reduction and sample clean up, separating proteins on the basis of their surface charge differences[1]. It is well known that a protein can adopt a local charge

[a] For Part CII, see ref. 29.

0021-9673/90/$03.50 

distribution at its surface, depending on the ionic strength and pH of the feed buffer, and is steered towards the ion-exchange resin containing complimentary charges by, amongst others, electrostatic forces. Biospecific and biomimetic chromatography represent highly tuned separation processes, often used at the latter stages of the chromatographic cascade for their high resolution. These chromatographic methods rely on distinct protein recognition of chemical or biological ligands, with the protein being driven by biospecific attractions that mimic *in vivo* phenomena observed, for example, in antigen–antibody or enzyme–substrate interactions.

Selectivity and efficiency in all chromatography modes depend strongly on the type of resin, the appropriate choice of sample buffer, water content, pH, displacing ions and ionic strength. Currently there are several hundred different ion-exchange resins now commercially available, from the traditional celluloses (Whatman diethylaminoethyl cellulose DE-52), cross-linked dextrans and agaroses (Pharmacia QAE-Sephadex A-25 and CM-Sepharose CL-6B), new synthetic methacrylate polymers (IBF Q-Trisacryl M), to various silica-based sorbents (Merck DEAE-LiChrospher 1000), designed for increased chemical and physical stability. In preparative chromatography, selection of the resin rests on the operational capabilities of the resin, its capacity for binding protein, its stability under high flow-rates and its cost. Ultimately, the criteria of resin productivity and throughput, for example, in terms of kilograms per hour per invested dollar, will dictate the use of a particular ion-exchange sorbent in process-scale purification of proteins. This requirement is in direct contrast to the criteria used for selecting resins for analytical purification, where demands of high selectivity and resolution are paramount. Bed compression, for instance, is a serious drawback in using the soft gels, such as the Sephadex based resins[2]. Most optimization studies have to date concentrated on these operational characteristics[3–5], and examined how these parameters influence the efficiency of the resin to adsorb protein.

It has been recently shown that the sorbent–protein interaction harnessed in the chromatographic purification also plays an important role in adsorption efficiency, in transport phenomena and in the binding kinetics[6,7]. At a process scale, effects such as (i) slow diffusion of the protein through the porous network of the sorbent, (ii) by tortuosity of the pore chambers, (iii) rotational masking of the protein affected by steric hindrance, and (iv) non-specific adsorption onto heterogeneous ligand/ionic sites, are exaggerated. The interplay of these effects can become detrimental to overall purity and throughput of the desired protein product[8–10]. Thus, the efficiency of the performance of different ion-exchange and dye-affinity sorbents, in terms of how quickly they adsorb the maximum amount of protein, and their kinetic behaviour towards biosolutes with different molecular features are characteristics that need to be optimized. This can be achieved only through a more lucid and complete understanding of their respective adsorption kinetics and mass transfer phenomena.

The experiments reported here have been designed to study the adsorption kinetics of dye-affinity gels and several ion-exchange resins, to allow a direct comparison of two different systems of selectivity that have similar association constants[11]. Mathematical models and literature correlations were also used to extract physicochemical parameters from the experimental results of two system modes, namely batch ion-exchange and affinity chromatography.

## THEORY

Adsorption of protein to a porous ion-exchange or dye-affinity sorbent entails the following macroscopic steps: (1) protein movement from the bulk, mobile phase to the sorbent surface layer; (2) protein transfer across a stagnant film layer surrounding the sorbent particles; (3) protein diffusion into the pores of the particles; (4) adsorption of protein to the solid phase.

Each of these steps contributes to the overall adsorption but the slowest and most significant step will be the rate-governing mechanism. External, bulk diffusion is often considered infinitely fast, resistance to film mass transfer can be minimal provided mixing is adequate, whilst pore diffusion can actually hinder adsorption, particularly if the protein size is large and the pore openings small[10].

The diffusion of complex species, such as proteins, which can change conformation and characteristics[12] is an intricate process. The transportation of a protein from the bulk fluid to the ligands inside the pores can be described mathematically, provided certain assumptions are made. For example, conformational changes of the protein are assumed to be negligible, both in the mobile and stationary phase. Secondly, the adsorption is often assumed to be highly specific, that is, no non-specific binding occurs to secondary sites. In addition, the flow of protein through the chromatographic bed is assumed to be ideal, with well distributed bulk flow, no channelling or no stagnant fluid around the resin particles or within its porous interior. Finally, the concentration of the protein is presumed to be same in the bulk, mobile phase and in the pores of the resin, that is, instantaneous equilibrium is achieved between the phases.

The mass balance equation for adsorption of protein to the stationary phase can then be written in the form,

$$\frac{\partial C}{\partial t} = D_a \frac{\partial C}{\partial x} - u\frac{\partial C}{\partial t} - \frac{\partial q}{\partial t} \tag{1}$$

where

$D_a$ = axial diffusion
$C$ = free protein concentration within solution
$u$ = superficial velocity
$q$ = protein concentration bound to the resin
$t$ = time
$x$ = distance along the bed

Analytical solutions to this equation have yet to be achieved. However, numerical techniques have been implemented to achieve a theoretical solution that is considered to simulate transport within the constraints of the previously stated assumptions. To achieve numerical solutions to equation 1, further assumptions from those mentioned above, have to be made. Firstly, axial diffusion is assumed to be infinitely fast[10,13] ($\partial C/\partial t = 0$) and secondly, mass transfer resistances are often considered to be negligible. Collectively the application of these assumptions thus permits the rate of change of adsorbed protein to be reduced to

$$\frac{dq}{dt} = k_1 C(q_m - q) - k_2 q \tag{2}$$

Eqn. 2, upon integration, yields

$$C(t) = C(\text{in}) - \frac{v(b + a)[1 - \exp(-2a(v/V)k_1 t]}{V[(b + \text{a})/(b - a)] - \exp(-2a(v/V)k_1 t)} \tag{3}$$

where

$a^2$ = $b^2 - C(\text{in})V/(vq_m)$
$b$ = $1/2(\text{C(in)}V/v + q_m + K_D V/v)$
$V$ = total buffer volume
$v$ = volume of resin
$k_1$ = first order rate constant
$q_m$ = maximum protein capacity
$C(t)$ = concentration of protein at any time
$C(\text{in})$ = initial protein concentration in bulk fluid
$k_2$ = reverse rate constant
$K_D$ = dissociation constant

The Langmuir isotherm has been derived for the most simple case where equilibrium exists at all points within and around the sorbent particles, so that $\partial q/\partial t \rightarrow 0$. Under these conditions, the equilibrium parameters are defined according to the familiar form

$$q = \frac{K_a q_m C}{1 + K_a C} \tag{4}$$

where $K_a$ = the association constant, $k_1/k_2$.

Inherent to eqn. 4, this approach has been earlier used by Chase[14] for kinetic studies on biospecific affinity adsorption. It should be kept in mind that eqns. 3 and 4 represent a very simplistic picture of a protein binding to an immobilized ligand. This approach takes no account of non-equilibrium effects, such as diffusional restrictions and film mass transfer. In addition, this model assumes unique protein binding to specific ligand, disregarding any heterogeneities, that may be more prevalent at a process level. Furthermore, as presented by Chase[14], the rate constants derived from eqn. 3 represent "lumped" parameters, that underestimate the speed with which protein will bind to the resins[15]. Arnold *et al.*[16], for example, have found that these constants are artificially small if the rate of mass transfer becomes comparable to the rate of binding. Sportmann *et al.*[17] and Hethcote and Delisi[28] have suggested that the rate of biospecific adsorption may be rate limiting, so that the kinetic rate constant measured by eqn. 3 may also not be indicative of the actual adsorption rate constant.

Development of kinetic equations for the binding of protein to an ion-exchange resin has followed similar approaches. Tsou and Graham[8] have developed a solution to the mass balance equations from the two-phase diffusion model[19]. This model assumes there are two effective films contributing to the overall resistance to solute diffusion. The overall flux of a protein is presumed to be concentration driven, a gradient existing between the concentration that would finally be in equilibrium, $C^*$, and the bulk concentration at any time, $C(t)$. The rate equation then becomes

$$\frac{dq}{dt} = \frac{3K}{r_0}[C(t) - C^*] \tag{5}$$

for which the final kinetic solution for the fractional obtainment of equilibrium, $F(t)$, becomes,

$$\ln[1 - F(t)] = -3\frac{Kt}{r_0}\left[\frac{V}{v} + \frac{1}{m''}\right] \tag{6}$$

where

$K$ = overall mass transfer coefficient
$r_0$ = radius of resin particle
$F(t) = \dfrac{(q^* - q)}{[q^* - q(\text{in})]}$
$m'' = \dfrac{(q^* - q)}{(C - C^*)}$

Thus, eqn. 6 predicts that the slope of $\ln[1 - F(t)]$ *versus* time, $t$, will be linear, with a slope proportional to $K$, and, depending on the rate controlling mechanism, the appropriate diffusivity can be calculated. Two cases are important here, namely when

(1) film diffusion controls adsorption where $D_p \propto \text{slope} \cdot r_0 \cdot (V/v)$ (7)

(2) pore diffusion controls adsorption where $D_f \propto \text{slope} \cdot r_0^2$ (8)

where

$D_p$ = pore diffusion
$D_f$ = film diffusion

Although eqns. 7 and 8 clearly oversimplify the mechanism of adsorption of proteins (species that are amphoteric and structurally diverse) to the charged ion-exchange resins, experimental values of protein diffusivities obtained[18,19] with this approach concur with the values of bulk diffusivities calculated from correlation.

Arve and Liapis[20] have produced a more sophisticated model of protein adsorption to affinity sorbents, by numerically solving the mass balance equation, eqn. 1, and incorporating mass transfer resistances and diffusional characteristics. Three cases of adsorption are applicable with this model.

Case 1: Local equilibrium exists, with Langmuirean behaviour prevailing, (*e.g.* eqns. 3 and 4). The adsorption is thus described solely by the equilibrium parameters, $K_a$, $q_m$ and the bulk diffusivity, $D_m$.

Case 2: Adsorption is described by a second order reversible rate equation, as in affinity adsorption, and pore diffusion is controlling.

Case 3: Adsorption is governed by an irreversible rate constant, for example, by very high affinity interactions with biometic and ion-exchange sorbents, and diffusion is again pore controlled.

The numerical solutions in this model are obtained from computational integration, using literature correlations[21,22] for initial parameter estimates, followed by an iterative procedure to obtain theoretical values for the protein diffusivity and rate constants. Solutions to cases 1 and 2 have previously been described using dye-affinity and biospecific affinity systems[23,24].

The applicability and adequacy of each model equation will depend on the

complexity of the crude mixture, the structural and conformational integrity of the protein to be purified and the homogeneity of the sorbents' macro- and micro-structure.

## EXPERIMENTAL

Human serum albumin (HSA), as a 21% solution, was kindly donated by Commonwealth Serum Laboratories (C.S.L., Melbourne, Australia). Lysozyme from hen egg white (dialysed and lyophilized), and ferritin, from horse spleen (isoelectrically isolated), were purchased from Sigma (St. Louis, MO, U.S.A.). Cibacron Blue F3GA was obtained from Serva (Heidelberg, F.R.G.). Buffer salts were obtained from Aldrich (Milwaukee, WI, U.S.A.). The Fractogels HW55, HW65 and HW75 were obtained from Merck (Darmstadt, F.R.G.); the Trisacryl M was from Australia Chemical Company (Melbourne, Australia); the Fast Flow Sepharose and the ion-exchange Sephadex resins were a gift from Pharmacia (Uppsala, Sweden). The properties of the chromatographic resins as given by the manufacturer are listed in Table I.

The experimental apparatus included a Model 2238 UV Spectrophotometer and a Model 2210 two-pen chart recorder from Pharmacia. Experimental data were analysed using an IBM PC with linkage to a VAX mainframe.

Batch experiments were performed using the bath system as previously described in our associated studies[7,24]. Typically, protein solutions ranging from 20 to 220 mg/ml were injected into a bath containing 20 ml of buffer and 0.1 g resin for IEC or 1.0 g for dye-affinity (dried on sintered funnel by vacuum). The bath was continuously stirred to maintain good mixing. The buffer used for IEC experiments was 5 m*M* phosphate, and a pH 6.0 was selected so that albumin would adsorb to the anion-exchanger (p*I* of HSA, 4.9). For the dye-affinity experiments, the buffer was 20 m*M* Tris–HCl, pH 7.8. In both cases the concentration of protein in solution was

TABLE I

PROPERTIES OF ANION EXCHANGE AND AFFINITY RESINS

| *Support* | *Particle size (μm)* | *Capacity for albumin (mg/ml)*[b] | *Exclusion limit (dalton)* |
|---|---|---|---|
| DEAE-Sephadex A-25 | 40–125[a] | 31[1] | 30 000 |
| Q-Sephadex A-25 | 40–125 | – | 30 000 |
| DEAE-Sephadex A-50 | 40–125[a] | 102[2] | 200 000 |
| DEAE-Sepharose FF | 45–165 | 110[3] | 4 000 000 |
| Q-Sepharose FF | 45–165 | 120[4] | 4 000 000 |
| DEAE-Fractogel 65 | 45–90 | 25[5] | 5 000 000 |
| DEAE-Trisacryl M | 40–80 | 105[6] | 10 000 000 |
| Q-Trisacyl M | | 145[7] | 10 000 000 |
| Fractogel HW55 | 32–63 | – | 1 000 000 |
| Fractogel HW65 | 32–63 | – | 5 000 000 |
| Fractogel HW75 | 32–63 | – | 50 000 000 |

[a] Dry bead diameter.

[b] 1 = Determined in 0.01 *M* Tris–HCl buffer pH 8.0; 2 = determined in 0.01 *M* Tris–HCl buffer pH 8.3; 3 = determined in 0.05 *M* phosphate buffer pH 9.0; 4 = determined in 0.05 *M* phosphate buffer pH 7.0; 5 = determined in 0.05 *M* Tris–HCl buffer pH 8.3; 6 = determined in 0.05 *M* Tris–HCl buffer pH 8.0; 7 = determined in 0.01 *M* Tris–HCl buffer pH 9.5.

measured continuously by UV spectrophotometry (280 nm), giving a concentration profile from the time protein was injected into the bath until steady state was achieved.

The porosities of the resins were measured using a Pharmacia FPLC LCC 500 system. Columns were packed with the sorbents and the elution volumes of (i) acetone, a suitable molecular weight analyte able to penetrate the pores of the resins, and (ii) thyroglobulin, a large globular protein, that should be partially excluded, were measured. The difference between the volumes provided data on the voidage of the columns, and hence a measure of the porosity of the resins, a physical property that can change with buffer conditions and therefore affect the exclusion property of the different sorbents. The densities of the swollen ion-exchange resins were measured in 5 m*M* sodium dihydrogenphosphate buffer, pH 6.0. The properties for the weak ion-exchange resins are listed in Table II.

TABLE II

POROSITY OF THE DEAE RESINS

| *Support* | *Porosity* | *Density (mg/ml)* |
|---|---|---|
| Sephadex A-25 | 0.39 | 1.5 |
| Sephadex A-50 | 0.75 | 1.1 |
| Sepharose FF | 0.65 | 1.4 |
| Fractogel HW65 | 0.28 | 1.3 |
| Trisacryl M | 0.49 | 1.2 |

## RESULTS AND DISCUSSION

### *Equilibrium measurements*

Adsorption isotherms were obtained from serial loading of protein solution onto the sorbents, in a batch, well mixed, system, as described previously[5]. These plots reflect the amount of protein bound to a resin once equilibrium with the protein solution is established. Fig. 1, taken from lysozyme and HSA adsorption experiments

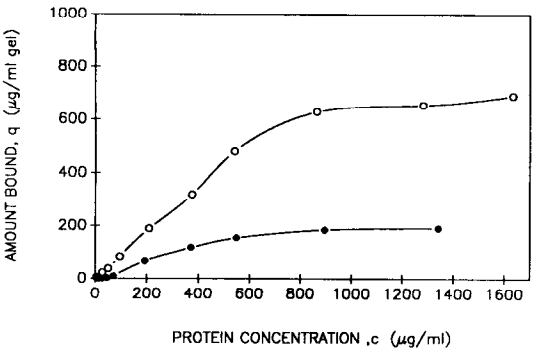


Fig. 1. Adsorption isotherm for the binding of lysozyme (○) and HSA (●) to the Fractogel HW65–Cibacron Blue F3GA support. Results generated from bath experiments with 1.0 g resin suspended in 20 ml of a 50-m*M* solution of Tris–HCl buffer, pH 7.8, temperature 35°C.

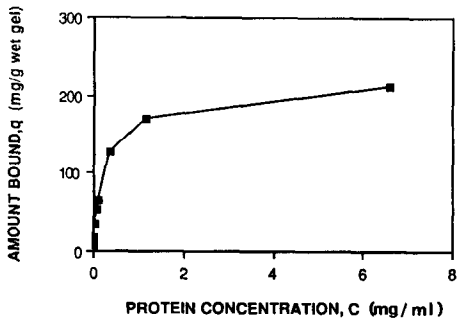


Fig. 2. Adsorption isotherm for the binding of HSA to Q-Sepharose FF resin. Results generated from bath experiments with 0.1 g resin suspended in 20 ml of a 5-m*M* solution of phosphate buffer, pH 6.0, temperature 25°C.

with the dye-affinity resin, Fractogel HW65–Cibacron Blue F3GA, demonstrates the effect of the ratio of pore to protein size. The smaller protein, lysozyme, with a hydrodynamic radius of 27 Å is anticipated to have easier access to the pores within the resin (exclusion limit of 5 000 000 dalton, and pore size approximately 190 Å, Table I), whilst the protein, HSA, with a larger molecular geometry (radius of 45 Å) should have restricted movement. Fig. 1 confirms this difference in accessibility, with the capacity of the Fractogel HW65–Cibacron Blue F3GA for HSA being significantly less. In addition, the adsorption curves of Fig. 1 suggest that the data approximately conform to Langmuirean behaviour. This adsorption behaviour allows estimation of the equilibrium parameters, such as the association constant, $K_a$, and the maximum capacity, $q_m$, parameters that are used as initial estimates of adsorption behaviour when equilibrium no longer prevails.

Figs. 2 and 3 show rectangular isotherms for the binding of HSA to the ion-exchange resin Q-Sepharose FF (Fast Flow) DEAE-Sephadex. As is evident from Fig. 2, the maximum capacity of Q-Sepharose FF for HSA was 170 mg/ml (compare with 0.18 mg/ml for Fractogel HW65–Cibacron Blue F3GA). The steeper initial slope reflects the higher affinity of interaction. Fig. 3 compares the capacity of two

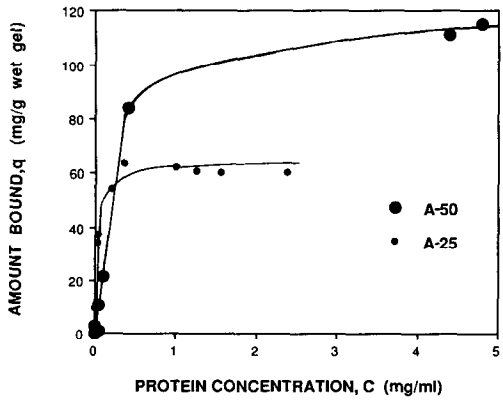


Fig. 3. Adsorption isotherm for the binding of HSA to DEAE-Sephadex A-25 and DEAE-Sephadex A-50 resin. Results generated from bath experiments with 0.1 g resin suspended in 20 ml of a 5-m*M* solution of phosphate buffer, pH 6.0, temperature 25°C.

DEAE-Sephadex-based resins with different pore sizes. DEAE-Sephadex A-25, with an exclusion limit of *ca.* 30 000 dalton will exclude albumin (molecular weight of 67 000 dalton) and thus adsorption is limited to the bead surface, whilst DEAE-Sephadex A-50, with the larger pores and higher surface area available to the protein, clearly binds more.

It is important to note here, that the maximum capacity calculated by this static, batch system, is much higher than that quoted by the manufacturer, see Table I (*e.g.* approximately 60 and 115 mg/ml, respectively). It should be kept in mind that experimental capacities depend on buffer conditions, pH, ionic strength (two conditions that are actually manipulated to affect elution) and mode of operation. Lower capacities are expected for packed beds where mixing is inferior, promoting a large film thickness and a resistance to mass transfer. That is, dynamic loadability (packed beds) is considered lower than static loadability (mixed baths). The soft gels, and in particular the Sephadex based resins, are known to compress under high flowrates in a packed bed, thus reducing their total surface area[2], and this pattern has also been seen in the Fractogel sorbents[24].

*Kinetic measurements*

*Dye-affinity experiments.* Concentration profiles of HSA binding to the Fractogel–Cibacron Blue F3GA, for varying pore size, are given in Fig. 4. The fastest rate and the greatest capacity are apparent for the Fractogel HW75, a matrix with large pores. The models of Arve and Liapis, Tsou and Graham, outlined in the theory were utilized and further validated here. Non-linear regression analysis, fitting eqn. 3, yielded first order rate constants, $k_1$, whilst iteration and parameter estimation are used to fit the solutions to cases 1 and 2 of Arve and Liapis, thus generating the apparent pore diffusivity and second order reversible rate constants. Fig. 5 compares the experimental concentration profile with the fitted theoretical curve of case 2, for the adsorption of HSA to the DEAE-Fractogel 65 resin.

The results for these two approaches are listed in Table III. The rates derived from eqn. 3 are comparable with those published by Chase[14] for the binding of HSA to Sepharose CL-6B Cibacron Blue F3GA. ($k_1$ = 0.09–0.02 *vs.* $k_1$ = 0.02 ml/mg · s). These rate constants appear to decrease with decreasing pore size, in the case of HSA,

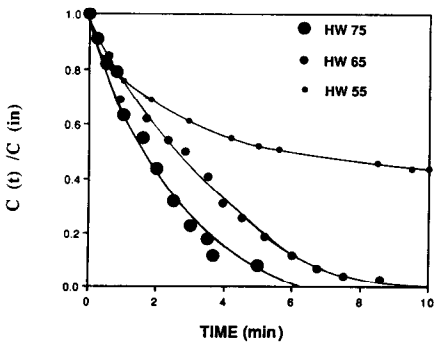


Fig. 4. Concentration time profiles of HSA adsorbing to the Fractogel HW55–, HW65– and HW75–Cibacron Blue F3GA supports. $C$(in) = 8, 9, 22 μg/ml respectively, for 1.0 g resin in 20 ml of a 50-m$M$ solution of Tris–HCl buffer, pH 7.8, temperature 35°C.

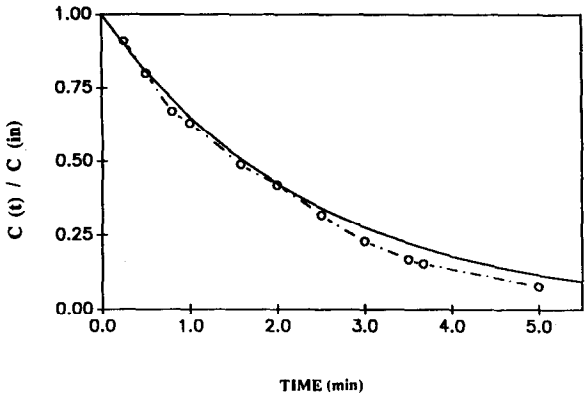


Fig. 5. Theoretical (———) and experimental (○---○) concentration curves of HSA adsorbing to the Fractogel HW65–Cibacron Blue F3GA supports. $C$(in) = 22 μg/ml, $D_p$ = 0.07 m²/s, $k_1$ = 0.1 ml/mg · s.

whilst lysozyme follows the opposite trend, indicating that the simple Chase model inadequately accounts for pore restrictions to mass transfer. It must be recognised that the rate constant as proposed by Case is a "lumped" parameter, incorporating all the factors that contribute to the overall adsorption process[15,16,24], and thus masks the true interaction rate. The adsorption process can be considered as a series of steps (see Theory), all of which should be accounted for in calculating the true interaction rate. The model of Arve and Liapis, on the other hand, gives rate constants that are higher than those of the Chase model, (see Table III) suggesting that they are more realistic representations of the rate of protein binding to an affinity resin. The rate constants, *per se*, arise from the interaction of protein with ligand, and therefore, should depend only on the class of protein and the type of ligand. Although diffusional restrictions have been accounted for in this model, there still appears a pore dependency.

*Ion-exchange experiments.* Proteins of different molecular sizes were used to study the effect of protein size on the kinetics of adsorption to the weak ion exchanger DEAE-Fractogel 65. The concentration profiles of Fig. 6 reflect the differences in

TABLE III

KINETIC PARAMETERS OF DYE-AFFINITY ADSORPTION

| *Protein* | *Support (Fractogel)* | *C (μg/ml)* | $k_1$ *(ml/mg · s)* | | |
|---|---|---|---|---|---|
| | | | *Eqn. 3* | *Arve and Liapis*[20] | *Chase*[14] |
| Lysozyme | HW55 | 5.0 | 0.096 | 5.0 | 0.020[a] |
| | HW65 | 7.0 | 0.041 | 1.8 | 0.020 |
| | HW75 | 11.6 | 0.023 | – | 0.020 |
| HSA | HW55 | 10.4 | 0.0008 | 0.10 | 0.012[a] |
| | HW65 | 4.9 | 0.0033 | 0.25 | 0.012 |
| | HW75 | 9.8 | 0.0100 | 0.50 | 0.012 |

[a] Adsorption of lysozyme in 50 m*M* Tris–HCl, pH 7.2, onto Sepharose CL-6B.

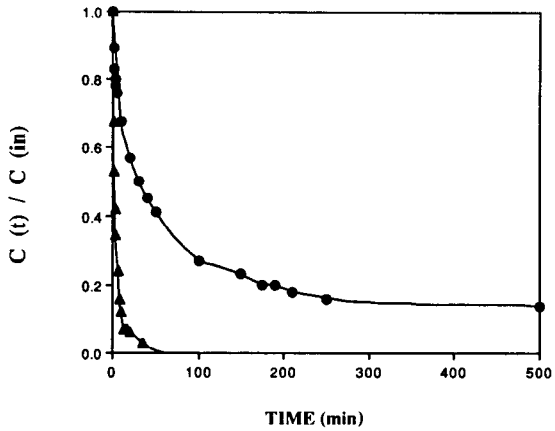


Fig. 6. Concentration–time profiles of HSA (▲) and ferritin (●) adsorbing to DEAE-Fractogel 65. $C(\text{in})$ = 104 μg/ml, for 0.1 g resin suspended in 20 ml of a 5 m*M* solution of phosphate buffer, pH 6.0, temperature 25°C.

molecular characteristics. For example, ferritin, with a molecular diameter two-fold larger than HSA (84:45 Å) adsorbs considerably slower, and because access to the Fractogel pores is expected to be more limited, less ferritin will bind [*i.e.* $C(t)/C(\text{in})_{\text{ferritin}} \rightarrow 0.2$, $C(t)/C(\text{in})_{\text{HSA}} \rightarrow 0.0$]. Experimental parameters, describing the kinetics of adsorption, can be extracted from these concentration profiles, using two mathematical approaches[18,20].

Following the approach of Tsou and Graham[18], concentration profiles such as shown in Fig. 6 were measured, with Figs. 7 and 8 being logarithmic transformation of these profiles. For both the DEAE-Fractogel 65 and the Q-Sephadex A-25, exponential behaviour is apparent from these transformed data. Since the exclusion limit of the Sephadex resin indicates that HSA will not penetrate the pores, it is likely that film diffusion will control the rate at which protein binds. If this behaviour is

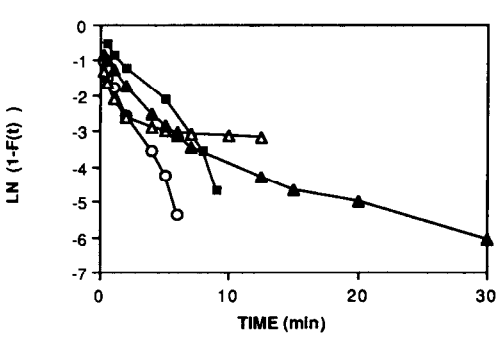


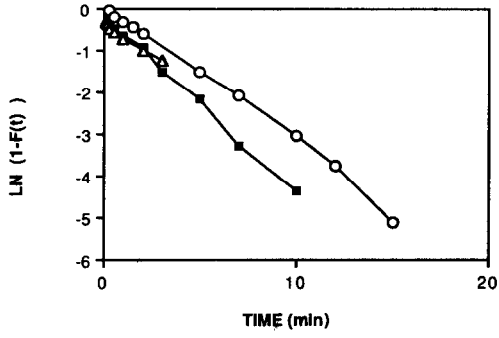


Fig. 7. Logarithmic plots of concentration profiles of HSA binding to DEAE-Fractogel 65. Each line represents sequential injection of a 200 mg/ml solution of HSA into the bath, containing 0.1 g resin in a 5-m*M* solution of phosphate buffer, pH 6.0, temperature 25°C.

Fig. 8. Logarithmic plots of concentration profiles of HSA binding to Q-Sephadex A-25. Each line represents sequential injection of a 200 mg/ml solution of HSA into the bath, containing 0.1 g resin in a 5-m*M* solution of phosphate buffer, pH 6.0, temperature 25°C.

TABLE IV

MODEL COMPARISONS FOR DEAE-FRACTOGEL 65

| *Protein* | *C* (*mg/ml*) | $D_p$ ($\times 10^{-11}$ $m^2/s$) | | $k_1$ (*ml/mg · s*) |
|---|---|---|---|---|
| | | *Ref. 18* | *Ref. 20* | |
| Ferritin[a] | 1 | 0.48 | 3.20 | 0.07 |
| | 104 | 0.10 | 0.05 | 0.30 |
| | 248 | 0.03 | 0.10 | 0.50 |
| HSA[b] | 22 | 0.06 | 6.0 | 0.5 |
| | 55 | 0.11 | 6.0 | 0.5–1.0 |
| | 104 | 0.08 | 6.0 | 0.5 |

[a] Bulk diffusivity = $3.4 \cdot 10^{-11}$ $m^2/s$.
[b] Bulk diffusivity = $6.1 \cdot 10^{-11}$ $m^2/s$.

occurring, then eqn. 7 is applicable for the binding of HSA to Q-Sephadex A-25, where slope $\propto D_p \cdot r_0$, whilst eqn. 8 will be appropriate for the DEAE-Fractogel 65/HSA system.

Using the model of Arve and Liapis[20], on the other hand, entails an iterative procedure, as opposed to a simple transformation, which yields theoretical estimates of the pore diffusivity and irreversible rate constants from experimental results. Table IV compares the results of the models. The model of Arve and Liapis predicts that the small protein, HSA, and low concentrations of the large protein, ferritin, are not pore restricted, their movement within the pore chambers simulating that in the bulk. It is likely that at low protein levels, the majority of ferritin binds exclusively to the surface of the resin. Thus, when iteratively fitting theoretical values to the experimental curve, bulk diffusivity remained unchanged. For higher concentrations of ferritin, the pore diffusivities as calculated from Tsou and Graham, Arve and Liapis are within the same orders of magnitude and are up to 30-fold smaller than the corresponding bulk diffusion. Similar results have been obtained for affinity binding of HSA to Fractogel HW65–Cibacron Blue F3GA, in which the pore to protein size ratio was comparable[6]. Furthermore, a trend is evident in the case of the model of Tsou and Graham, towards a decrease in protein diffusion with increasing concentration of protein injected into the bath. This trend has previously been predicted for adsorbent binding to carbon particles[25]. This behaviour is not however apparent for HSA. In examining the results for HSA, it appears that the effective diffusivities predicted by the two models differ. The model of Tsou and Graham indicates a 100-fold decrease in protein diffusivity, as calculated from eqn. 8, whilst the model of Arve and Liapis model predicts no change in diffusion from the original estimate of the bulk diffusion. In addition, the treatment of Tsou and Graham results in little difference in pore diffusion between the geometrically different proteins, however further experimental results from the adsorption of carbonic anhydrase and ferritin to various ion-exchange resins have demonstrated otherwise[26].

Table IV shows a comparison of the irreversible rate constants, $k_1$, extracted from the solutions to case 3 of Arve and Liapis. The results for ferritin binding to DEAE-Fractogel 65 for various concentrations, show that this irreversible rate constant increases with increasing protein concentration. This behaviour is consistent

with enzyme kinetic theory which predicts an increase in the rate of binding to the sorbent as more protein is added to the feedstock solution[27]. The equilibrium model of Tsou and Graham for ion exchange, in contrast, has predicted much slower diffusion for HSA binding to the DEAE-Fractogel 65, than the model of Arve and Liapis.

## CONCLUSIONS

The above results, demonstrating adsorption capacities and binding kinetics of two different chromatographic systems, have confirmed that protein movement into the porous sorbent particles commonly used in analytical chromatography, can lead to significant restrictions in ligand accessability in preparative applications. Ion-exchange resins, with greater capacities for protein than the dye-affinity resins, show very fast kinetics for the smaller proteins as demonstrated from the measurement of the overall rates of adsorption. Kinetic rate constants have also been calculated in attempt to ascertain the efficiency of the resins. The equilibrium model of Chase was found to underestimate the rate constants of the affinity adsorption process, whilst the pore diffusion models of Arve and Liapis gave rate constants that were higher, yet pore dependant. In addition, rate constants describing the ion-exchange process were found to be concentration dependent with the large protein, ferritin.

## ACKNOWLEDGEMENTS

The support of the Australian Research Council and the Monash University Research Committee is gratefully acknowledged. A.J. is a post-graduate scholar associated with the Commonwealth Serum Laboratories.

## REFERENCES

1 A. Hodder, M. T. W. Hearn and M. I. Aguilar, *J. Chromatogr.*, 443 (1988) 97.
2 K. K. Unger and R. Janzen, *J. Chromatogr.*, 373 (1986) 227.
3 G. Ganetsos, *J. Chromatogr.*, 411 (1987) 81.
4 S. Ghodbane and G. Guiochon, *J. Chromatogr.*, 452 (1988) 209.
5 T. S. Katoh, T. Kambayashi, R. Deguchi and F. Yoshida, *Biotechnol. Bioeng.*, 20 (1978) 267.
6 F. B. Anspach, A. Johnston, H.-J. Wirth, K. K. Unger and M. T. W. Hearn, *J. Chromatogr.*, 476 (1989) 205.
7 Cs. Horváth and J.-M. Engasser, *Biotechnol. Bioeng.*, 16 (1974) 900.
8 A. M. Lenhoff, *J. Chromatogr.*, 384 (1987) 285.
9 V. Kasche and B. Galunsky, in T. C. J. Gribrau, J. Visser and R. J. F. Nivard (Editors), *Affinity Chromatography and Related Techniques*, Elsevier, Amsterdam, 1982, pp. 93–111.
10 I. A. Webster, *Biotechnol. Bioeng.*, 25 (1983) 2479.
11 Y. S. Ghim and H. N. Chang, *Ind. Eng. Chem. Fundam.*, 21 (1982) 369.
12 M. T. W. Hearn, A. Hodder and M. I. Aguilar, *J. Chromatogr.*, 448 (1988) 95.
13 W. Kopaciewicz, S. Fulton and S. Y. Lee, *J. Chromatogr.*, 409 (1987) 111.
14 H. A. Chase, *J. Chromatogr.*, 297 (1984) 179.
15 H. A. Chase, in A. I. Liapis (Editor), *Proceedings of the 2nd International Conference on Fundamentals of Adsorption, Santa Barbara, CA, 1986*, Engineering Foundation, New York, 1987, pp. 155–165.
16 F. H. Arnold, H. W. Blanch and C. R. Wilke, *Chem. Eng. J.*, 30 (1985) 25.
17 J. R. S. Sportmann, J. D. Liddil and G. S. Wilson, *Anal. Chem.*, 55 (1983) 771.
18 H-S. Tsou and E. E. Graham, *AIChE J.*, 31 (1985) 1945.
19 E. E. Graham and C. H. Fook, *AIChE J.*, 28 (1982) 245.
20 B. H. Arve and A. T. Liapis, *AIChE J.*, 33 (1987) 179.

21 R. E. Treybal, in J. V. Brown and M. Eichberg (Editors), *Mass Transfer Operations*, McGraw-Hill, Tokyo, 1981, p. 144–152.
22 M. E. Young, P. A. Carroad and R. L. Bell, *Biotechnol. Bioeng.*, 12 (1980) 947.
23 F. B. Anspach, A. Johnston, H.-J. Wirth, K. K. Unger and M. T. W. Hearn, *J. Chromatogr.*, 476 (1989) 205–225.
24 A. Johnston, *M.(Sc.) Thesis*, Monash University, Melbourne, 1988.
25 E. Furya, H. Ikeda and Y. Takeucha, in A. I. Liapis (Editor), *Proceedings of the 2nd International Conference on Fundamentals of Adsorption, Santa Barbara, CA, 1986*, Engineering Foundation, New York, 1987, pp. 235–240.
26 A. Johnston and M. T. W. Hearn, in preparation.
27 J. E. Bailey and D. F. Ollis, in B. J. Clark, B. Tokay and J. W. Bradley (Editors), *Biochemical Engineering Fundamentals*, McGraw-Hill, Tokyo, 1977, pp. 92–100.
28 H. W. Hethcote and C. Delisi, *J. Chromatogr.*, 248 (1982) 183.
29 M. T. W. Hearn, in J. Rivier and G. Marshall (Editors), *Peptides '90*, ESCOM Publ., San Diego, CA, 1990, in press.